Fundamental study on quality improvement of cement-based ground improvement using fine bubbles

Yukari Kinoshita[1], *Shuichi* Shimomura[1*], *Masakazu* Matsumoto[2], and *Yousuke* Mizutani[3]

[1] Department of Architecture and Architectural Engineering, College of Industrial Technology, Nihon University, Chiba, Japan
[2] Department of Applied Molecular Chemistry, College of Industrial Technology, Nihon University, Chiba, Japan
[3] Kanematsu Suntech Corporation, Japan

Abstract. In cement-based ground-improvement methods, the potential difference between soil and cement particles may result in the formation of electrical aggregates, which can hinder the uniform mixing of soil and cement slurry in situ. Consequently, the strength of the improved soil may not be desirable. As a countermeasure, surfactants can be used to prevent aggregate formation by adsorbing onto cement particles to provide steric hindrance and electrical repulsion. However, cost and environmental challenges remain. By contrast, fine bubbles carry negative charges in aqueous solutions and are expected to exhibit effects similar to those of surfactants when mixed with cement slurry. Furthermore, fine bubbles are expected to function similarly to ball bearings. Therefore, this study investigates whether fine bubbles can be used as a substitute for surfactants. First, surface potential measurements confirmed that cement particles with adsorbed fine bubbles exhibited reduced surface potential. Additionally, funnel tests confirmed the improved flowability of the cement slurry. Finally, using a small-scale deep-mixing machine, we confirmed that the mixing resistance of a soil–cement slurry decreased with the addition of fine bubbles. These results indicate that fine bubbles can effectively enhance mixing efficiency and flowability, serving as a viable alternative to surfactants.

1. Introduction

For cement-treated ground, characteristics such as significant variations in the physical constants of the soil-improvement body are problematic in the design and construction of these structures. A possible cause of these variations is the significant amount of large fines, which results in highly viscous soil–cement slurry during the solidification process. This is due to the hydration reaction of the cement-based solidifying material (hereafter, 'solidifying material'), which hinders the sufficient agitation and mixing of the soil–cement slurry. A previous study [1] reported the properties of a soil–cement slurry and indicated that its viscosity changed over time and that the condition of false solidification was governed by the unique properties of the soil to be treated. In general, clay is negatively charged, which creates an environment that allows adhesion to the calcium ions of the cement component in the solidifying material. In this study, we evaluate a solidification method that mixes the solidifying material into a cohesive soil with few polyvalent ions, as shown in Fig. 1(a), and a method that mixes the solidifying material into a cohesive soil with many polyvalent ions, as shown in Fig. 1(b). When the mixture contains few polyvalent ions, the possibility of positive-ion exchange is low. This results in a low level of adhesion with calcium ions in the solidifying material, thus impeding the formation of aggregated bodies. By contrast, mixtures containing many polyvalent ions show greater adhesion between the cohesive soil and solidifying material, resulting in the formation of aggregated bodies and a network of aggregated bodies that sustain water in the soil to increase the viscosity of the soil–cement slurry.

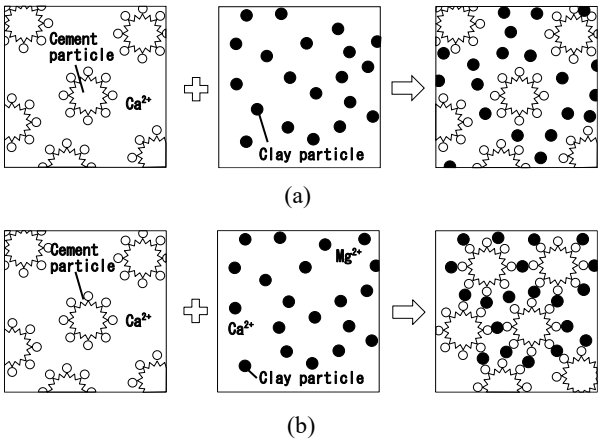

Fig. 1. Outline of aggregation: (a) few polyvalent ions and (b) Many polyvalent ions.

Adding a surfactant during the preparation of cement slurry has been shown to be effective in reducing the variations in the physical properties of stabilised soil. This method promotes a homogeneous dispersion of the slurry within the medium via the repulsive force of the

* Corresponding author: ciyu22131@g.nihon-u.ac.jp

surfactant, in addition to the mechanical force of the mixer.

Meanwhile, fine bubbles have recently been investigated extensively. Because fine bubbles are known to be negatively charged in solution, we hypothesise that the resulting electrical property can inhibit the aggregation of soil–cement slurry. Therefore, in this study, we measured the ζ-potential of fine bubbles and a cement slurry containing fine bubbles to verify the electrical mechanism underlying the aggregation inhibition. Furthermore, we fabricated a device to directly measure the agitation resistance of a soil–cement slurry and confirmed the effectiveness of fine-bubble inclusion in inhibiting aggregate formation.

2. Electrical Characteristics

2.1 Overview of ζ-Potential

Fig. 2 shows a schematic diagram of the ζ-potential. If negatively charged particles are present, then positively charged ions will surround those particles to form a Stern layer. Around this Stern layer, the diffuse layer forms a mixture of ions with positive and negative charges. Owing to the shear forces generated by the movement of the particles, some of the ions traverse with the particle while some others depart from the particle within the diffuse layer, thus resulting in the formation of a boundary surface (slipping plane) between them. The potential in the slipping plane is known as the ζ-potential.

Currently, a methodology for directly measuring the surface potentials of particles does not exist. Therefore, the ζ-potential is generally regarded as the surface potential.

2.2 Method for Measuring ζ-Potential

The ζ-potential was examined via microscopic electrophoresis [2]. In electrophoresis, an electric field is applied to a solvent containing particles such that particles with a positive charge approach the negative electrode, while particles with a negative charge approach the positive electrode. Subsequently, the ζ-potential is obtained via image processing to monitor and measure the ease of movement per unit time. This measurement method included the following steps:

1. The specimen is placed in a beaker together with ion-exchanged or pH-adjusted water. The mixture is agitated for 1 min using a glass rod to prepare the measurement solution.
2. The measurement solution is placed in the measurement equipment.
3. Measurements are performed continuously until a specified amount of image data is obtained.
4. Particles from the obtained image data are monitored manually to obtain the ζ-potential.

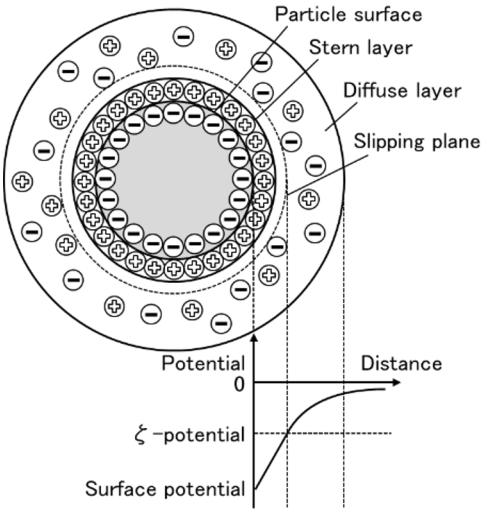

Fig. 2. Outline of ζ-potential.

2.3 Measurement Conditions

The measurement conditions are listed in Table 1. The specimens were characterised as kaolin clay, Kasaoka clay, and a solidifying material. Cases 1 and 2 provide the measurement conditions for the kaolin and Kasaoka clays, respectively. Case 3 provides the measurement conditions for the solidifying material, while Case 4 provides the conditions when a polycarboxylic acid-based surfactant (hereafter, 'surfactant') is added to the medium of Case 3, with the amount of surfactant equal to 10% of the solidifying material's mass.

Case 5 includes only fine bubbles, whereas Case 6 entails the addition of a solidifying material to Case 5. Fine bubbles were generated using the hydraulic-impact method [3]. This method generates fine bubbles by jetting a solution containing dissolved gas through multiple nozzles, thus causing the streams to collide with each other (Fig. 3). Nitrogen was used as the dissolved gas in the experiments.

Table 1. Conditions for ζ potential measurement.

Case	Specimen	Solvent	Water volume	Remarks
Case 1	Kaolin Clay	Ion-exchanged water	300 cc	Kaolin Clay 0.8g
Case 2	Kasaoka Clay			Kasaoka Clay 0.8g
Case 3	Solidifying material			Solidifying material 1.5g
Case 4	Solidifying material +Polycarboxylate-based dispersant	pH-adjusted water		Solidifying material 1.5g Polycarboxylate-based dispersant 0.15g
Case 5	Fine bubbles			-
Case 6	Solidifying material+ fine bubbles			Solidifying material 1.5g

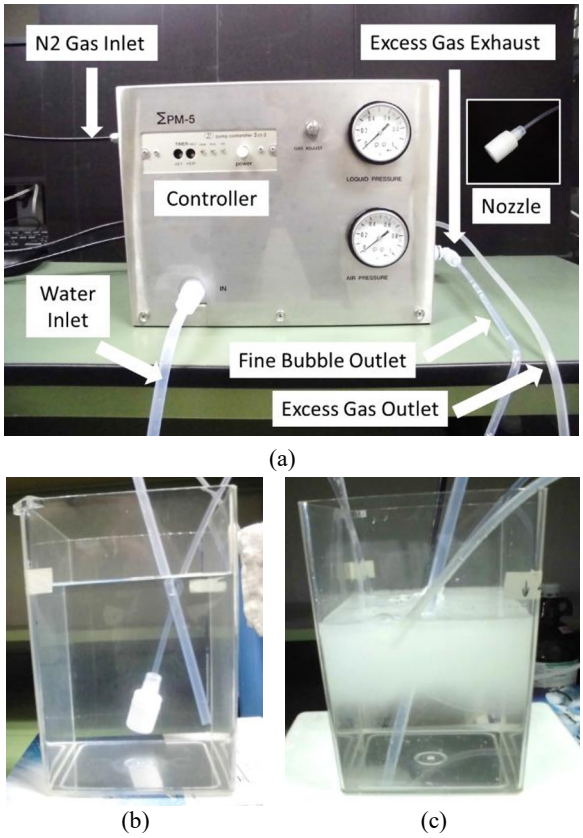

Fig. 3. Fine bubble generator (Water hammer method): (a) fine bubble generator, (b) before generation and (c) during generation.

Fig. 4 and Table 2 show the grain-size distribution and physical properties of the soil, and Table 3 presents the characteristics of the surfactant.

In general, cohesive soil particles are negatively charged, and cement particles are positively charged; as the pH environment changes, the potential of the fine particles changes as well [4,5]. During cement-based ground improvement, the treated ground may become alkaline because of the solidifying material.

Preliminary measurements revealed that the solution, prepared by adding the solidifying agent to ion-exchanged water (pH 5.6), had a pH of 12.4. Based on the pH data obtained, the soil particles were measured using ion-exchanged and pH-adjusted water to model the conditions within the treated ground. The pH was adjusted to 12.4 by dissolving sodium hydroxide in ion-exchanged water.

2.4 Measurement Results

Fig. 5 shows the ζ-potential of the kaolin-clay particles in Case 1. In ion-exchanged water, particles may be positively or negatively charged; however, in pH-adjusted water, the potential is lower, and all particles are negatively charged. This trend is similar to the results for Kasaoka clay in Case 2, as shown in Fig. 6

Fig. 7 presents the ζ-potentials of solely the solidifying-material particles and the solidifying-material particles in a medium to which surfactant was added, which correspond to Cases 3 and 4, respectively. The solidifying-material particles are positively charged, and the addition of the surfactant reduces the potential, thus causing the particles to be negatively charged.

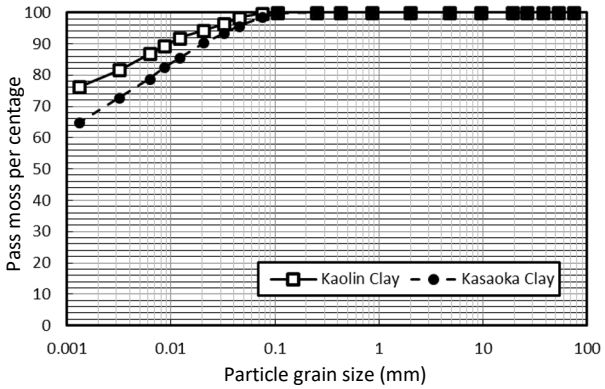

Fig. 4. Particle grain size distribution of test soil.

Table 2. Test soil characteristics.

Clay type	ρ (g/cm^3)	Ip
Kaolin clay	2.748	30.2
Kasaoka clay	2.710	45.1

Table 3. Surfactant characteristics.

Appearance	Liquid of light brown color
Specific gravity	About 1.29
pH value	About 8
Molecular weight	About 12000
Solubility	Soluble in water

These results indicate that, similar to the use of polycarboxylate-based surfactants, the use of fine bubbles causes both the cohesive-soil and solidifying-material particles to become negatively charged. This suggests that aggregate formation is prevented by electrostatic repulsion.

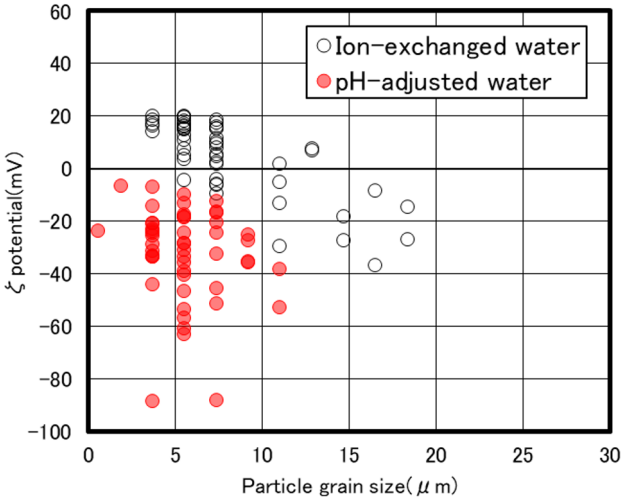

Fig. 5. Potential of kaolin clay particles.

Fig. 8 shows the measurement results for Case 5 (fine bubbles only) and Case 6 (fine bubbles with adsorbed solidifying-material particles). The results for Case 3 (solidifying-material particles only) are shown in the same figure for comparison. In Case 6,

measurements were performed on particles in which the solidifying material had adsorbed onto the fine bubbles (Fig. 9). Fig. 8 shows that the fine bubbles were negatively charged. Additionally, the potential of the solidifying-material particles adsorbed onto the fine bubbles decreased, which corresponds to the results obtained for the solidifying-material particles with surfactant added.

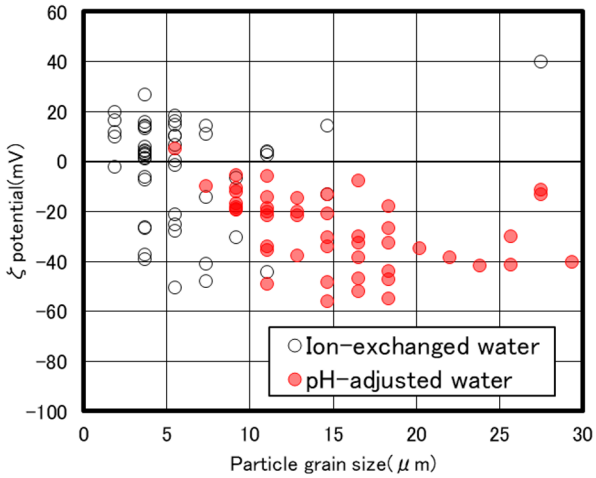

Fig. 6. Potential of Kasaoka clay particle.

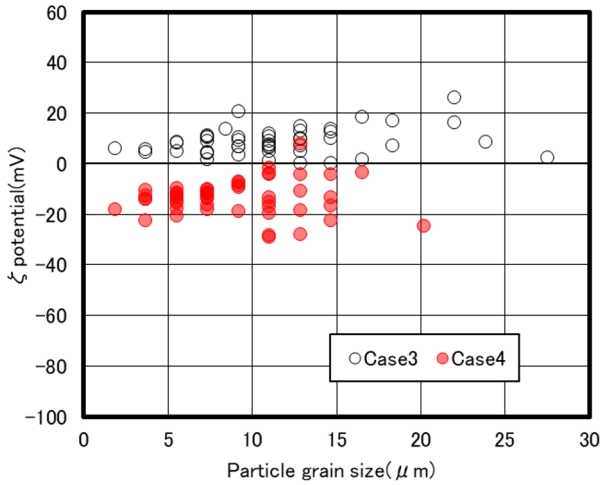

Fig. 7. ζ-potentials of solidifying-material particles and those with added dispersant.

3. Measurement of Mixing Resistance

3.1 Mixing-Resistance Measuring Device

Fig. 10a shows the mixing section, and Fig.10b shows the fabricated mixing-resistance measuring device. The mixing blade was designed as an approximately 1/4-scale model of 600 mm diameter blades, which are typically used in the deep-mixing method. The mixing resistance of the soil–cement slurry was evaluated by installing a flange-type torque meter between the rod and mixing blade to directly measure the torque variations during mixing. During the measurements, the rod and mixing section were rotated but not shifted vertically. As the torque meter was integrated into the rotating assembly, we attached a data logger to the rod and configured it to rotate together with the assembly.

3.2 Experimental Conditions and Procedure

Table 4 shows the experimental conditions. The mixing resistance was measured for two types of slurries: plain soil–cement slurry and soil–cement slurry with added fine bubbles. For the fine bubbles, N_2 gas was used. All conditions other than the addition of bubbles were fixed. For three cases in total, the mixing resistance was measured twice for each case. Fine bubbles were introduced into the cement slurry using the shearing method, as shown in Fig.9.

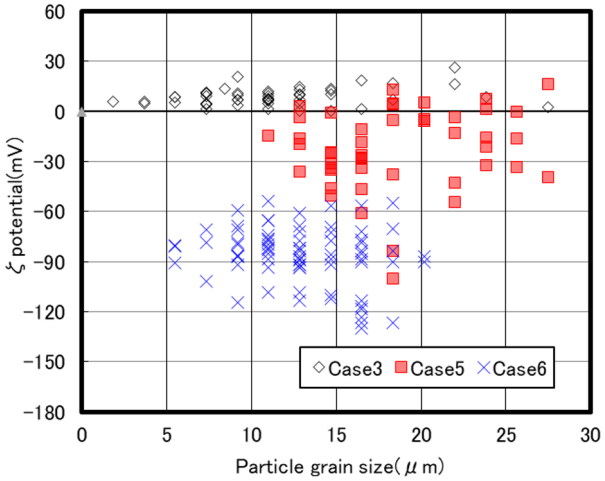

Fig. 8. ζ-Potentials of fine bubbles and solidifying-material particles.

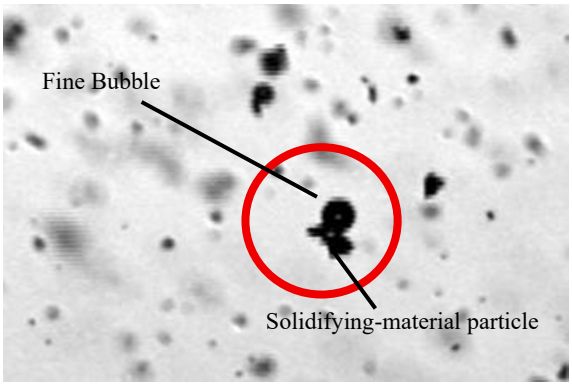

Fig. 9 Solidifying-material particles adsorbed onto fine bubbles.

Fig. 11 shows the time schedule for the cases involving fine-bubble injection. The experimental procedure is outlined as follows:

1. Clay and water were weighed and mixed using a hand mixer to prepare a soil sample.
2. The no-load mixing resistance and mixing resistance of the soil sample were measured. The rotational speed was set to 30 rpm, the sampling frequency to 10 Hz, and the measurement duration to 10 min.
3. A cement slurry was prepared, and a P-funnel test was conducted.
4. Fine bubbles were directly injected into the cement slurry. The injection duration was 5 min, and the total injection volume was 250 cc (flow rate: 50 cc/min).
5. A P-funnel test was performed on a fine bubble-containing cement slurry.

6. The soil sample and fine bubble-containing cement slurry were mixed to prepare the soil–cement slurry.
7. The mixing resistance of the soil–cement slurry was measured.

The procedure described above outlines the process for cases involving fine-bubble injection. The procedures for the cases without additives and those with surfactant were identical, except for the bubble-injection step and the frequency of the P-funnel tests. As the mixing resistance of the soil–cement slurry increased over time, the timing of each operation synchronised across all cases, regardless of whether fine bubbles were injected. The P-funnel test was conducted twice for the fine-bubble cases (before and after injection), whereas it was conducted only once for the cases without additives.

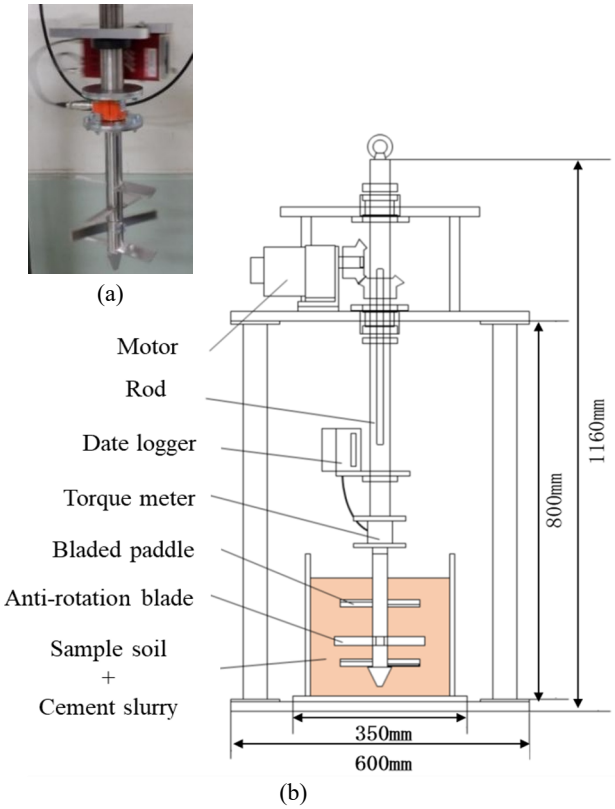

Fig. 10. Agitation resistance measurement system: (a) mixing section and (b) schematic of agitation resistance measurement system.

3.3 P-funnel Test Results

Table 5 presents the P-funnel test results, which confirmed that for N_2 bubbles, the fluidity improved compared with the cases without additives.

3.4 Measurement Results of Mixing Resistance

Figs. 12 and 13 show the mixing-resistance measurement results for each soil type. Results from the first trial are shown as representative data. Notably, a higher absolute torque value indicates a higher mixing resistance. For both the kaolin and Kasaoka clays, the mixing resistance increased in the order of N_2 bubbles < no additive. These results confirm that, consistent with the electrical properties discussed in Section 2, the inclusion of fine bubbles inhibits the formation of electrically induced aggregates in the soil–cement slurry, thereby improving the fluidity.

Table 4. List of test conditions.

Case	Cement slurry: Additive	Cement slurry: Dosage	Cement slurry: Cement content (g)	Cement slurry: Water content (ml)	Sample soil	Sample soil: Water content (ml)	Water content (ml)	Number of tests
A	No additive	-	1597	958 (W/C=60%)	Kaolin Clay	8630	6540 (water content 85%)	2
B	N_2 Bubbles	250cc (50cc/min)	1589	953 (W/C=60%)	Kasaoka Clay	9343	6540 (water content 70%)	2

Table 5. P-funnel test results.

Cement slurry		Flow time (s)	
Case	Additive	Without additive	With additive
A-1	No additive	10.53	-
A-2	No additive	11.09	-
B-1	N_2 bubble	10.81	9.13
B-2	N_2 bubble	10.19	9.28

Periodic fluctuations were observed in the time histories of the torque values across all test results. This cycle continued for approximately 160 s. Because this phenomenon is independent of the sample presence or additive type, we presumed that it was caused by factors inherent to the experimental apparatus or torque meter.

A possible cause is the slight eccentricity of the motor or shaft gears, which may generate periodic peaks and troughs in the shaft torque.

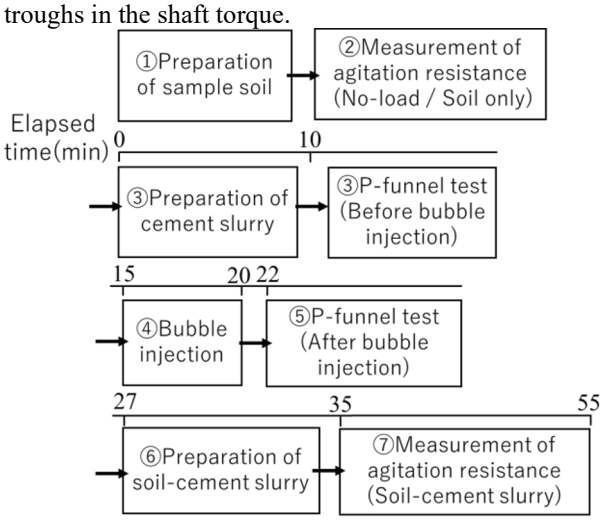

Fig. 11. Time schedule (case with fine bubbles).

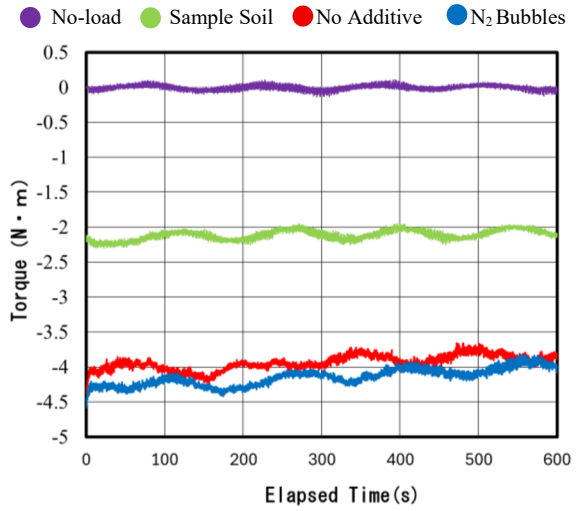

Fig. 12. Measurement of agitation resistance in Kaolin Clay (first run for each case).

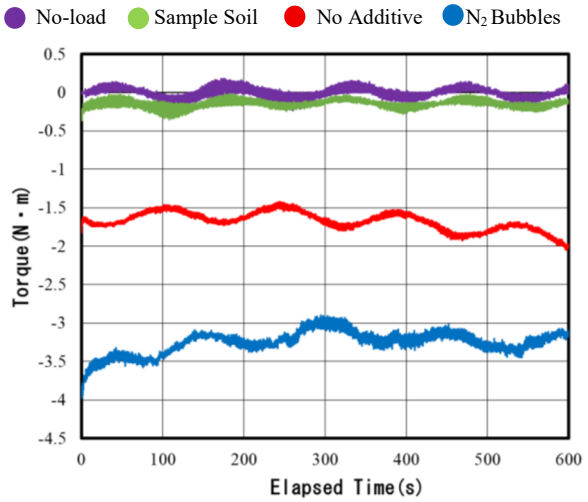

Fig. 13. Measurement of time history of agitation resistance in Kasaoka Clay (first run for each case).

Fig. 14 presents the average torque values calculated over the measurement period and shows a comparison of the averages of two trials for both the kaolin and Kasaoka clays. The improvement in fluidity due to fine-bubble addition was more pronounced in the Kasaoka clay than in the kaolin clay. Additionally, whereas the Kasaoka clay exhibited almost no mixing resistance as a soil sample alone, its resistance increased significantly upon mixing with the cement slurry.

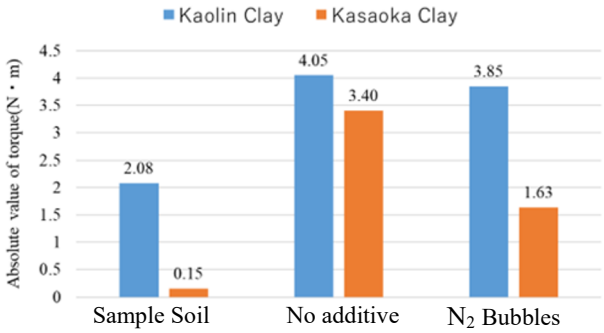

Fig. 14. Comparison of average stirring resistance by soil specimen.

4. Elemental Analysis

The effect of fine-bubble inclusion on improving the fluidity of the soil–cement slurry varied depending on the soil sample. Therefore, focusing on the elemental composition of the clays, the elemental content of each clay was measured using inductively coupled plasma mass spectrometry. The measurement results are listed in Table 6. Kasaoka clay contains higher levels of sodium and potassium compared to kaolin clay. Compared to Kaolin clay, Kasaoka clay exhibits significantly more prominent aggregate formation after the addition of the solidifying agent. This is presumed to be due to its high sodium (Na) and potassium (K) content, suggesting that the effectiveness of adding fine bubbles is greater in soils with more pronounced aggregate formation.

Table 6. Comparison of elemental content by ICP-MS analysis.

Target elements	Concentration in solution (mg/L)	
	Kasaoka Clay	Kaolin Clay
Na	5.100	2.30
Si	0.960	1.06
S	0.560	0.53
K	0.810	0.53
Ca	1.600	1.70
Mg	0.320	0.32
Al	0.410	0.31
Ti	0.056	0.41
Fe	0.270	0.36

5 Conclusions

This study focused on fine bubbles and verified their ability to inhibit aggregation in soil–cement slurries through their electrical properties. This verification was conducted by measuring the electric potential of clay

particles, a solidifying material, and fine bubbles, as well as by measuring the mixing resistance of the soil–cement slurry. The key findings are summarised below.

1. ζ-potential measurements using micro-electrophoresis revealed that, under pH conditions simulating improved ground, the clay particles were negatively charged while the solidifying-material particles were positively charged. Thus, aggregate formation is attributable to the electrical properties.
2. The addition of fine bubbles caused the solidifying-material particles to become negatively charged. This suggests the possibility of electrostatic repulsion occurring between the solidifying-material and clay particles.
3. Measurements of mixing resistance of the soil–cement slurry revealed that the fluidity improved by the addition of fine bubbles. This effect varied depending on the clay type.
4. The effect of fine-bubble addition on improving the fluidity of the soil–cement slurry might be affected by the sodium and potassium contents of the clay particles.

In future studies, we plan to perform further testing by varying the quantity, size, and gas type of fine bubbles. Additionally, we intend to investigate the differences in the effects caused by variations in the soil samples. It should be noted that although a reduction in mixing resistance is achieved as a result of the suppression of aggregate formation and the improved flowability of the soil-cement slurry, the uniform mixing of the soil and the solidifying material has not been directly evaluated. In future studies, direct evaluation methods, such as observing the soil-cement mixture using an electron microscope, will be necessary.

References

1. K. Aoyama, K. Miyamamori, T. Wakiyama, D. Kikuchi, The influence of physico-chemical property on improved soil character. J. JSCE **721**/VI-157, 207–219 (2002).
2. M. Takahashi, Zeta potential of microbubble aqueous solutions: Electrical properties of the gas–water interface. J. Phys. Chem. B **109**, 21858–21864 (2005).
3. M. Matsumoto, T. Fukunaga, K. Onoe, Polymorph control of calcium carbonate by reactive crystallization using microbubble technique. Chem. Eng. Res. Des. **88**, 1624–1630 (2010).
4. D. J. A. Williams, K. P. Williams, Electrophoresis and zeta potential of kaolinite. J. Colloid Interface Sci. **65**, 79–87 (1978).
5. C. Schwer, E. Kenndler, Electrophoresis in fused-silica capillaries: The influence of organic solvents on the electroosmotic velocity and the zeta potential. Anal. Chem. **63**, 1801–1807 (1991).